CENTER FOR TRANSPORTATION INFRASTRUCTURE AND SAFETY

Mechanical Characterization of Enamel Coated Steel Bars

by

Fujian Tang, Genda Chen, Jeffery S. Volz, Richard K. Brow, and Michael Koenigstein

A National University Transportation Center at Missouri University of Science and Technology

Disclaimer

The contents of this report reflect the views of the author(s), who are responsible for the facts and the accuracy of information presented herein. This document is disseminated under the sponsorship of the Department of Transportation, University Transportation Centers Program and the Center for Transportation Infrastructure and Safety NUTC program at the Missouri University of Science and Technology, in the interest of information exchange. The U.S. Government and Center for Transportation Infrastructure and Safety assumes no liability for the contents or use thereof.

Technical Report Documentation Page

1. Report No.	2. Government Accession No.	3. Recipient's Catalog No.
NUTC R208		

4. Title and Subtitle	5. Report Date
Mechanical Characterization of Enamel Coated Steel Bars	December 2012
	6. Performing Organization Code

7. Author/s	8. Performing Organization Report No.
Genda Chen	Project # 00018130

9. Performing Organization Name and Address	10. Work Unit No. (TRAIS)
Center for Transportation Infrastructure and Safety/NUTC program Missouri University of Science and Technology 220 Engineering Research Lab Rolla, MO 65409	11. Contract or Grant No. DTRT06-G-0014

12. Sponsoring Organization Name and Address	13. Type of Report and Period Covered
U.S. Department of Transportation Research and Innovative Technology Administration 1200 New Jersey Avenue, SE Washington, DC 20590	Final
	14. Sponsoring Agency Code

15. Supplementary Notes

16. Abstract

In this study, the corrosion process of enamel-coated deformed rebar completely immersed in 3.5 wt.% NaCl solution was evaluated over a period of 84 days by EIS testing. Three types of enamel coating were investigated: pure enamel, 50/50 enamel coating, and double enamel. Surface condition of the enamel coatings that were intentionally damaged prior to corrosion tests was visually examined at different immersion times. After 84 days of testing, the damaged coating areas were characterized by SEM, and the corrosion products on and adjacent to the damaged areas were collected and analyzed by XRD. Corrosion initiated at the damaged locations with no undercutting of the coating observed. The 50/50 enamel coating had the least corrosion resistance, due to its interconnected pore structure, and prior damage drastically reduced the corrosion resistance of pure and double enamel coated rebar.

17. Key Words	18. Distribution Statement
Reinforcement, corrosion, enamel	No restrictions. This document is available to the public through the National Technical Information Service, Springfield, Virginia 22161.

19. Security Classification (of this report)	20. Security Classification (of this page)	21. No. Of Pages	22. Price
unclassified	unclassified	14	

Form DOT F 1700.7 (8-72)

Corrosion Behavior of Enamel Coated Steel Rebar by EIS

Fujian Tang[1,a], Genda Chen[1,b], Jeffery S. Volz[1,c], Richard K. Brow[1,d], and Michael Koenigstein[2,e]

[1]Missouri University of Science and Technology, Rolla, MO 65409-0030, U.S.A.

[2] Pro-Perma Engineered Coatings, Hypoint, Rolla, MO 65401, U.S.A.

[a]ftkr7@mst.edu, [b]gchen@mst.edu, [c]volzj@mst.edu, [d]brow@mst.edu, [e]mkoenigstein@pro-perma.com.

Keywords: Corrosion resistance; Enamel coating; EIS; SEM/EDS; XRD.

Abstract

In this study, the corrosion process of enamel-coated deformed rebar completely immersed in 3.5 wt.% NaCl solution was evaluated over a period of 84 days by EIS testing. Three types of enamel coating were investigated: pure enamel, 50/50 enamel coating, and double enamel. Surface condition of the enamel coatings that were intentionally damaged prior to corrosion tests was visually examined at different immersion times. After 84 days of testing, the damaged coating areas were characterized by SEM, and the corrosion products on and adjacent to the damaged areas were collected and analyzed by XRD. Corrosion initiated at the damaged locations with no undercutting of the coating observed. The 50/50 enamel coating had the least corrosion resistance, due to its interconnected pore structure, and prior damage drastically reduced the corrosion resistance of pure and double enamel coated rebar.

Introduction

Reinforcement corrosion is one of the main causes of premature deterioration for concrete structures in aggressive environments. In the U.S., approximately $8B is spent on highway bridges for corrosion mitigation every year [1]. Presently, fusion bonded epoxy coating and hot-dip galvanized coating [2-4] are the most common methods of protecting rebar from corrosion. Porcelain enamel has excellent chemical stability, good corrosion resistance and durability in various environments such as high temperature, acid or alkaline conditions [5]. An innovative vitreous ceramic coating has recently been introduced by Pro-Perma Engineered Coatings for reinforcing steel in concrete structures for enhancement of steel-concrete bond and improved corrosion resistance. Earlier applications of this coating have been investigated by the Corps of Engineers [6]. However, the long-term performance and deterioration mechanism of the enamel coating has not been determined previously.

The main objective of this study is to investigate the corrosion behavior of three types of enamel-coated steel bars by electrochemical impedance spectroscopy (EIS) tests. Emphasis is placed on the effects of prior damage on the coating performance and corrosion process around damage areas.

Experimental

Enamel Coatings and Test Samples. The steel used in this study is standard rebar with a diameter of 13 mm and the chemical composition shown in Table 1. Three different coatings were used, pure enamel, 50/50 enamel, and double enamel, respectively. The typical batch composition of a pure enamel coating is shown in Table 2 [7]. This composition was selected because it contains ZrO_2 that is

known to improve the durability of glasses exposed to alkaline environments including cement. The 50/50 enamel consists of 50% pure enamel by weight and 50% calcium silicate that was directly obtained by mixing with Portland cement. The double enamel has an inner pure enamel layer and an outer 50/50 enamel layer. Prior to enameling, steel rebar was polished with grit paper and cleansed with water-based commercial solvents. The cleansed steel rebar was then dipped into porcelain slurries and then heated to approximately 850 °C for 10 minutes to fuse the melted glass to the steel surface.

Table 1 Chemical composition of steel rebar

Element	C	Si	Mn	P	S	Cr	Mo	Ni	Co	Cu	V	Sn	Fe
Wt.%	0.38	0.18	1.00	0.12	0.06	0.10	0.07	0.20	0.01	0.37	0.02	0.03	97.40

Table 2 Chemical composition of alkali borosilicate glasses [7]

Element	SiO_2	B_2O_3	Na_2O	K_2O	CaO	CaF_2	Al_2O_3	ZrO_2	MnO_2	NiO	CoO
Wt.%	44.0	19.3	15.8	2.8	0.1	4.7	4.6	5.3	1.5	1.0	0.9

A total of 30 rebar samples were prepared: 3 uncoated and 27 coated with three types of enamel, 9 samples for each type of coating. Each rebar sample was sectioned into 89 mm lengths and a copper wire was connected electrically at one end of the rebar. PVC tubes containing epoxy resin were used to cover the two exposed ends, as shown in Fig. 1. Therefore, the actual length of steel potentially exposed to the corrosive environment was approximately 50.8 mm long.

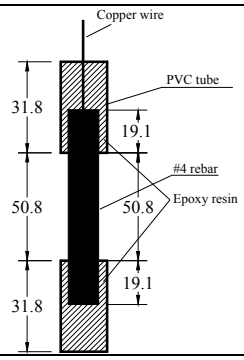

Fig. 1 Rebar samples (unit: mm)

Uncoated

50/50 enamel

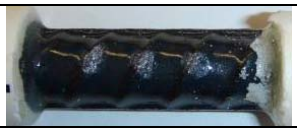

Pure enamel

Double enamel

Fig. 2 Prior damage induced by impact

To study the effect of coating damage on corrosion resistance, 6 out of 9 coated rebar of each type were pre-damaged with ASTM G14 impact tests. Two damage extents were considered, 3 samples with 6 damage points and 3 samples with 12 damage points as shown in Fig. 2.

EIS Tests. All samples were immersed in 3.5 wt.% NaCl solution over a period of 84 days with EIS tests conducted after various immersion times. A typical three-electrode setup was used in this study. A 25.4mm×25.4mm×0.254mm platinum sheet functions as a counter electrode, a saturated calomel electrode (SCE) as a reference electrode, and the rebar sample as the working electrode. EIS measurements were taken at a sampling rate of 5 points per decade under an applied sinusoidal potential wave of 10 mV in amplitude with frequency ranging from 100 kHz to 0.005 Hz around a stable open-circuit potential.

XRD and SEM/EDS Tests. The phase composition and microstructure of enamel coatings, and the oxide layer of uncoated rebar were investigated by X-ray diffraction (XRD) and scanning electron microscopy (SEM) coupled to an energy dispersive spectrometer (EDS). XRD was conducted on the

surface of as-received and enamel coated rebar samples, and SEM/EDS measurements were performed on longitudinal cross sectional samples 20 mm long. Each was polished with silicon carbide papers with grits of 80, 180, 320, 600, 800 and 1200.

Forensic Studies of Tested Samples. Surface conditions of uncoated and enamel coated samples with damage points were recorded after an immersion time of 7 days, 28 days, 56 days and 84 days, respectively. After 84 days of testing, cross sectional slices 3 mm thick were cut from the damage areas of both uncoated and enamel coated rebar samples. The slices were polished using silicon carbide papers with grits of 80, 180, 320, 600, 800 and 1200 as well. SEM was performed on these slices to investigate the development of corrosion. In addition, the corrosion products around the damage areas were also collected and analyzed by XRD.

Results and Discussions

Coating Characterization. The phase composition of the oxide layer of uncoated rebar samples is shown in Fig. 3a. Magnetite (Fe_3O_4) and Maghemite (Fe_2O_3) are the two main oxides on the surface of as-received steel rebar. The phase compositions of three enamel coatings are presented in Figs. 3b-3d. The amorphous pure enamel coating is dominated by SiO_2. Crystalline Ca-silicate and mullite phase were detected in both 50/50 and double enamel coatings. Both phases are present in the Portland cement added to the enamel slurry to produce the 50/50 enamel coating. The similar phase distribution in the 50/50 enamel and double enamel coatings are consistent with the similar microstructures noted in the respective layers shown in Fig. 4.

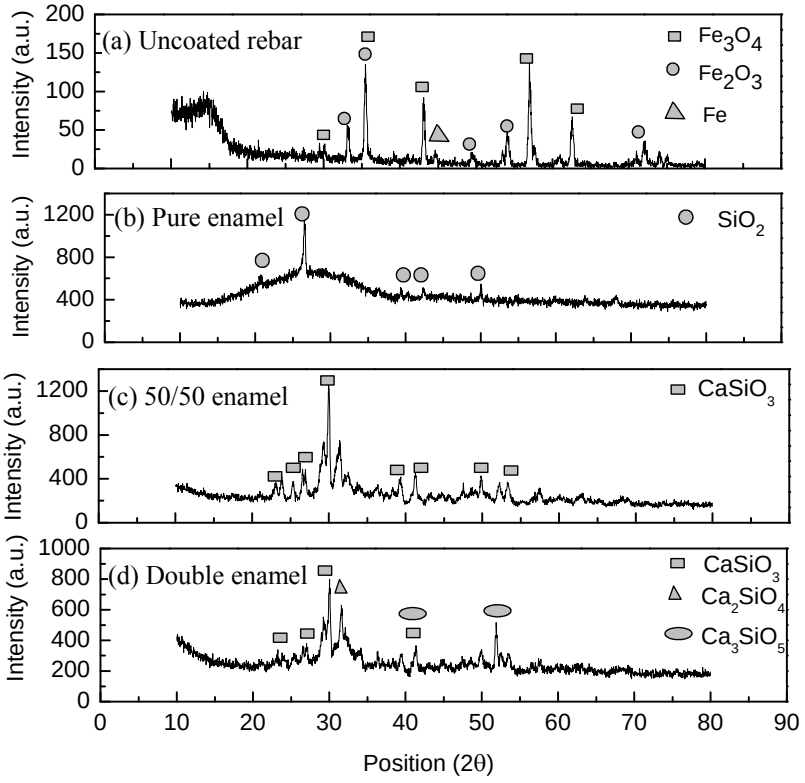

Fig. 3 XRD patterns of steel rebar and three enamel coatings

Coating Microstructure Prior to Corrosion. Fig. 4 shows the longitudinal cross sectional SEM images and the elemental analyses of uncoated and enamel coated rebar samples. As shown in Fig. 4a, the surface of the uncoated rebar has a thin iron oxide layer of approximately 40 μm. The oxide layer is relatively uniform at ribs and between the ribs. The pure enamel coating (see Fig. 4b) has bubbles of approximately 200 μm in diameter that are distributed between rebar ribs. These bubbles were formed when gases were trapped in the melted glass during firing, which is a normal result of the enameling process. In the pure enamel, Na, O, Si, Ca, Al and K are the basic elements detected. The 50/50 enamel coating (see Fig. 4c) has a complex structure with trapped bubbles in the residual glassy phase along with continuous regions of calcium silicate particles. The 50/50 enamel coating has significantly more calcium particles than the pure enamel coating. The double enamel coating has small bubbles of approximately 50 μm in diameter in the thick coating area between ribs. Both the 50/50 and double enamel have a similar amount of principal elements such as O, Si and Ca. However, relatively less calcium is present in the double enamel. In addition, ribs have significant influences on the thickness of all three types of enamel coatings. It is observed that the coating at ribs is always thinner than that between the ribs. The maximum coating thicknesses between the ribs are approximately 600 μm, 500 μm, and 600 μm for the pure, 50/50 and double enamel, respectively.

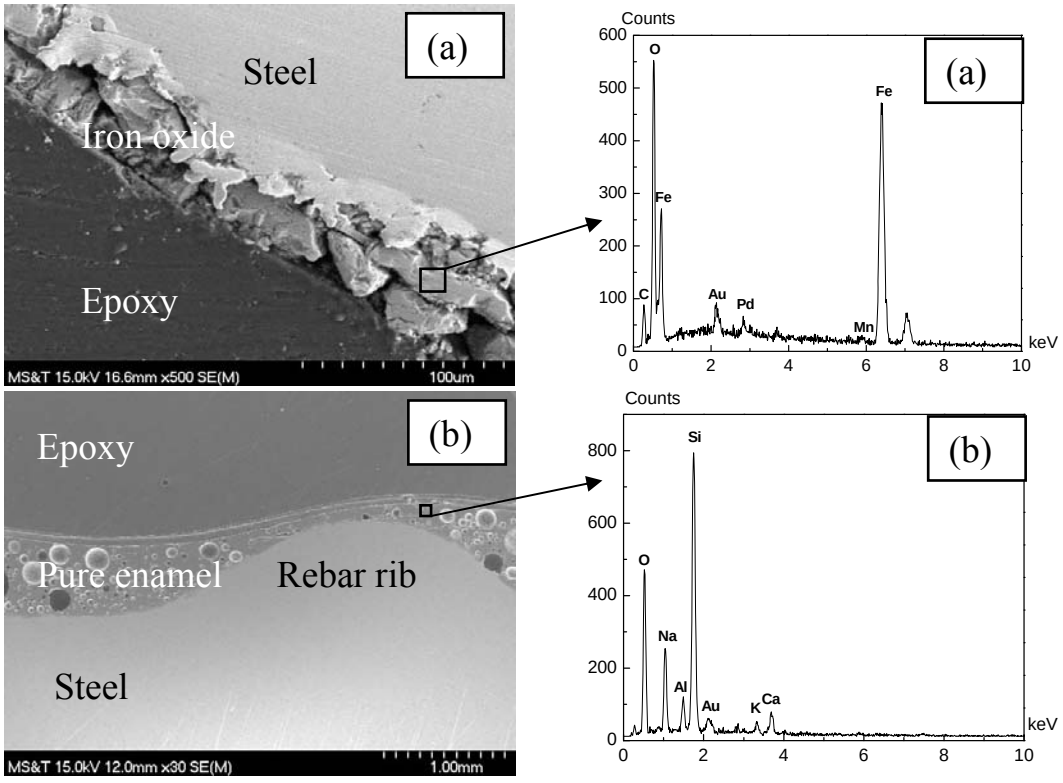

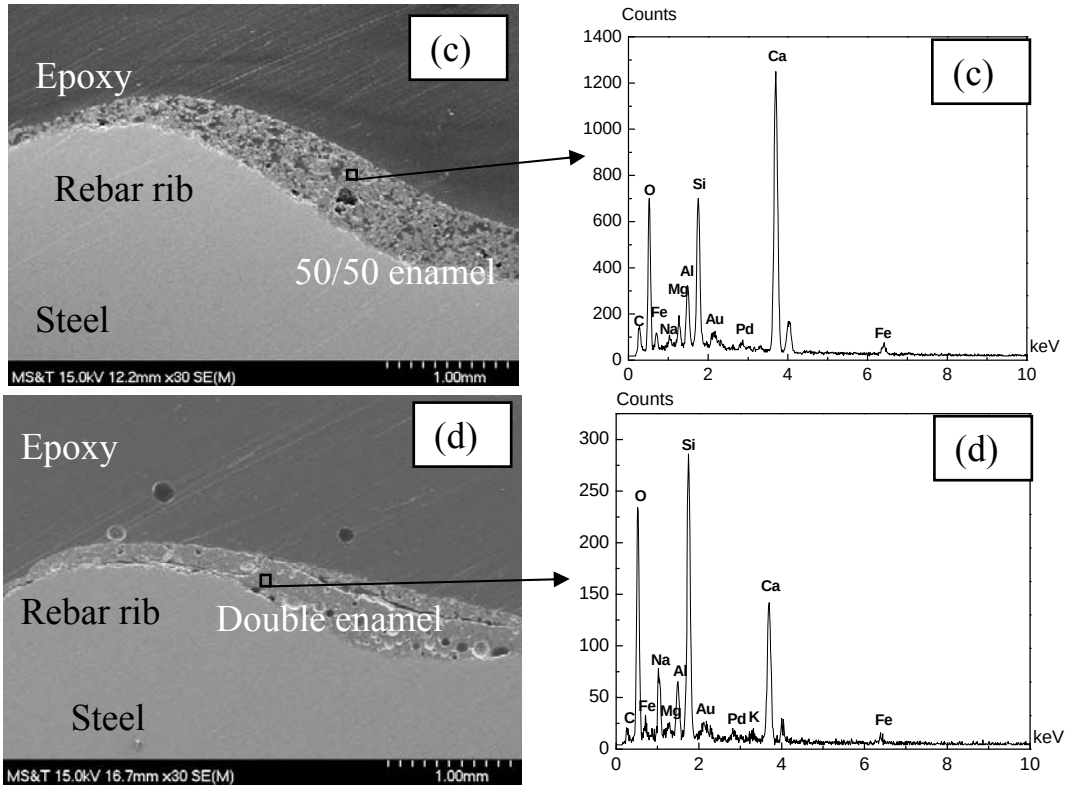

Fig. 4 SEM images and elemental analysis of (a) uncoated, (b) pure enamel, (c) 50/50 enamel, and (d) double enamel coated rebar

EIS Test Results. Fig. 5 shows a representative set of test data from three steel rebar samples coated with double enamel that were immersed in 3.5 wt.% NaCl solution for 84 days. It can be observed from Fig. 5 that all Nyquist plots are represented by a depressed arc and all Bode diagrams are similar. The depressed arc represents the characteristics of a constant phase element (CPE) that is attributed to the rebar surface inhomogeneity as a result of the coating variation and impact-induced damage.

The corrosion test system can be modeled with an equivalent electrical circuit (EEC) that consists of a resistor in series with two CPE-R units as shown in Fig. 6. The series resistance R accounts for the salt solution resistance, whereas the other elements refer to the two layer capacitance (CPE_2) at the steel-enamel interface of coated rebar or at the steel-oxide interface of uncoated rebar, and the charge transfer resistance (R_2). The parameters R_1 and CPE_1 were introduced to simulate high frequency loops that may be associated with the dielectric properties of enamel coatings.

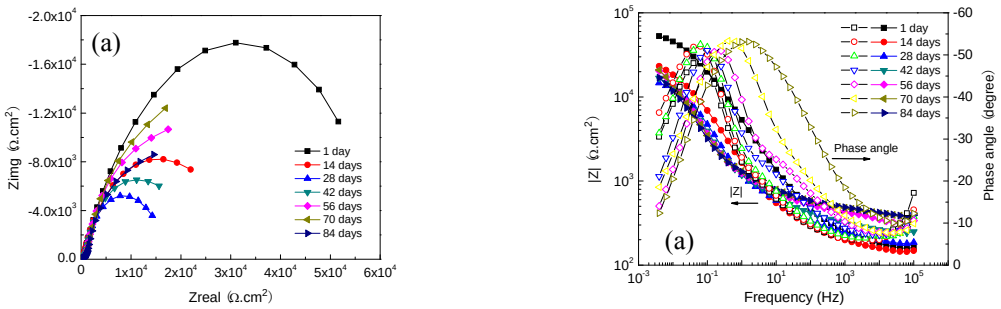

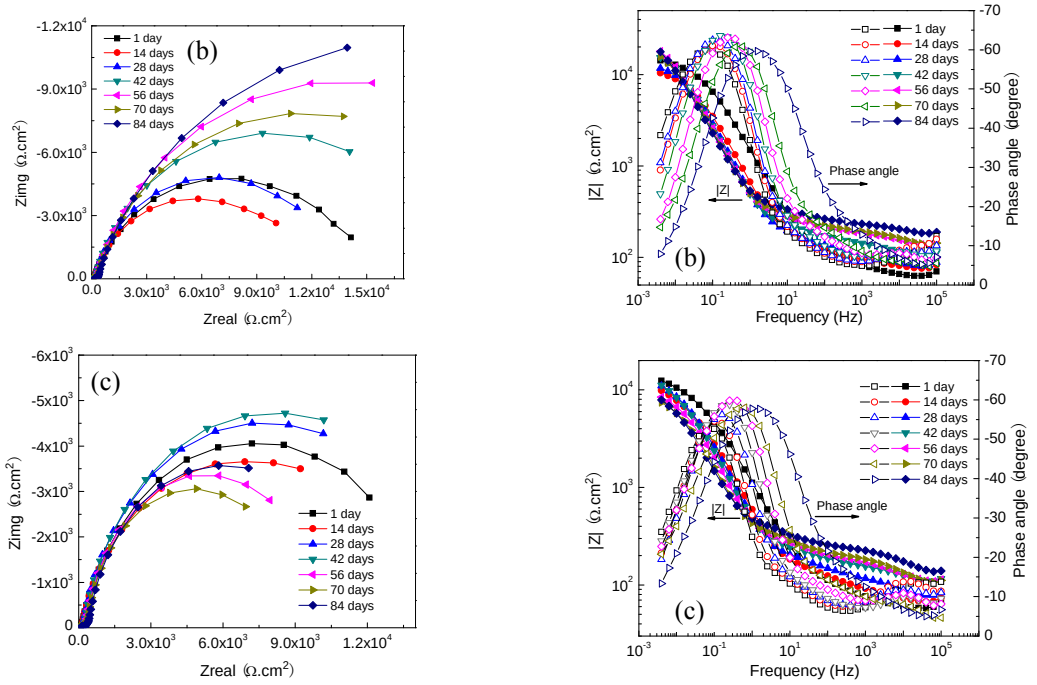

Fig. 5 Nyquist and Bode diagrams of double enamel coated rebar in 3.5 wt.% NaCl solution with: (a) 0 damage points (b) 6 damage points and (c) 12 damage points

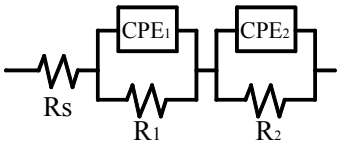

Fig. 6 Equivalent electrical circuit

The interfacial property between the passive film/enamel coating and their substrate steel is mainly reflected by the EEC parameters CPE_2 and R_2. In general, the CPE_2 parameter Q_2 does not represent any capacitor when $n_2 \neq 1$. However, an effective capacitance of the CPE_2-R_2 unit can be defined by [8].

$$C_{eff} = Q_2^{1/n_2} R_2^{(1-n_2)/n_2} \quad (1)$$

Fig. 7 presents the change in charge transfer resistance over time for the uncoated and three enamel coated steel rebar samples in 3.5 wt.% NaCl solution. As shown in Fig. 7a, the charge transfer resistance of uncoated steel rebar changed little over time except between 30 and 40 days. The overall average resistance is approximately 2000 $\Omega.cm^2$. As shown in Figs. 7b - 7d, with undamaged enamel coating, the charge transfer resistance of coated rebar decreased rapidly in the beginning and eventually approached values of approximately 1.5×10^4 $\Omega.cm^2$, 0.6×10^4 $\Omega.cm^2$, and 2.2×10^4 $\Omega.cm^2$ for pure, 50/50, and double enamel coatings, respectively. The number of damage points has little effect on the charge transfer resistance of pure and 50/50 enamels. For the double enamel, the larger the number of damage points, the smaller the charge transfer resistance. For the 50/50 enamel coated samples, the difference in charge transfer resistance between the undamaged and damaged samples decreased with immersion time. This result is likely due to the penetration of chloride ions through the porous enamel coating as shown in Fig. 4c; corrosion occurred around the damage points and other coating areas, but was dominated by the latter after a long immersion time.

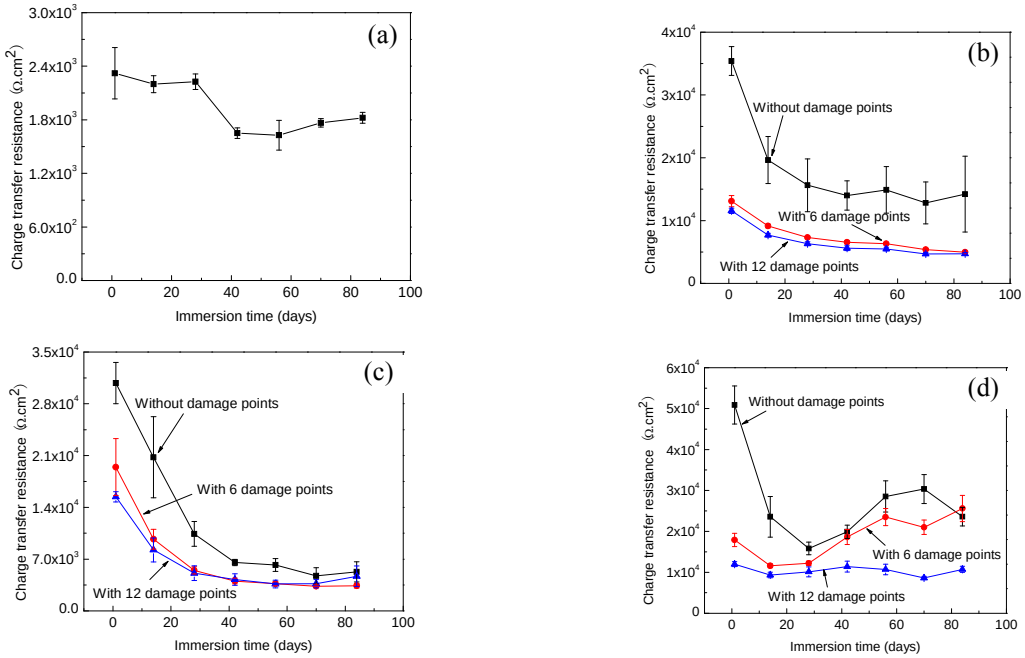

Fig. 7 Charge transfer resistance evolution for: (a) uncoated, (b) pure enamel coated, (c) 50/50 enamel coated, and (d) double enamel coated steel rebar

Fig. 8 shows the effective interfacial capacitance between the enamel coating/oxide layer and their substrate steel as a function of immersion time. For uncoated steel samples, the effective capacitance increased with immersion time from 1×10^{-2} F/cm^2 to 3.4×10^{-2} F/cm^2 likely due to the dissolved oxide layer into the 3.5 wt.% NaCl solution. For enamel coated samples, the effective capacitance increased rapidly in the first 15 days and then slowly in the following 70 days. As indicated in Figs. 8b and 8d, the influence of the number of damage points can be observed for pure and double enamel coated samples. The larger the number of damage points, the larger the effective capacitance. However, for 50/50 enamel coated rebar, little difference was seen as a function of the number of damage points. For undamaged coatings, the effective capacitances of coated rebar approached $(2.3\pm0.03)\times10^{-3}$ F/cm^2, $(5.3\pm1.5)\times10^{-2}$F/cm^2, and $(1.21\pm0.03)\times10^{-3}$F/cm^2 for pure, 50/50, and double enamel, respectively.

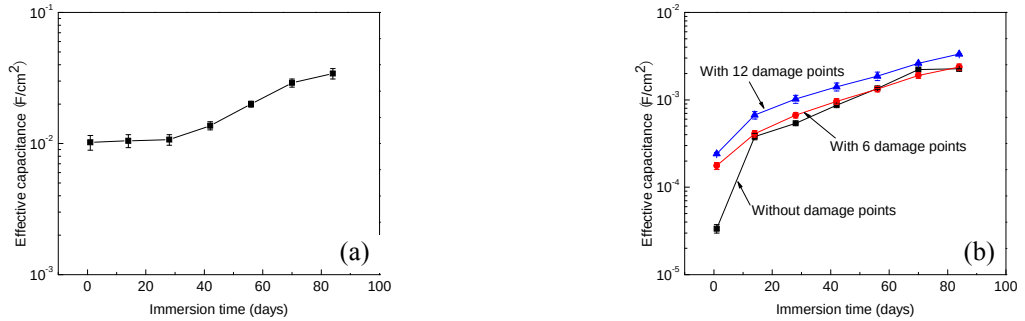

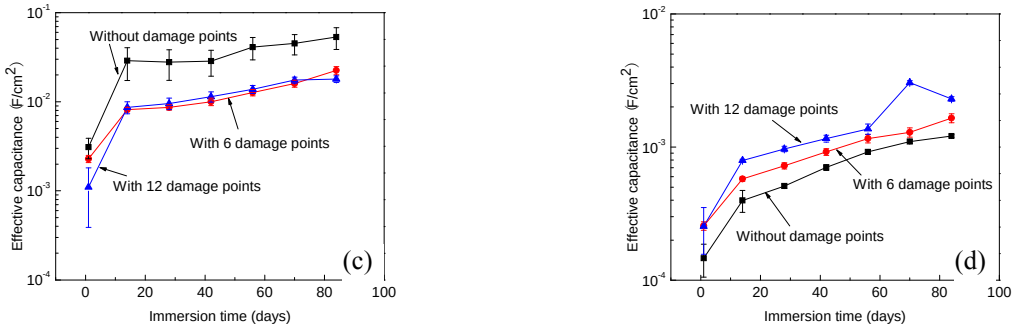

Fig. 8 Effective interfacial capacitance between coating/passive film and their substrate steel for: (a) uncoated, (b) pure enamel coated, (c) 50/50 enamel coated, and (d) double enamel coated steel rebar

Investigation of Corroded Samples. Table 3 shows the surface conditions of one uncoated and three coated rebar samples after being completely immersed in 3.5 wt.% NaCl solution for various times. Overall, uniform corrosion was observed on the uncoated rebar, while localized corrosion was observed on the three enamel coated samples. For the pure and double enamel coated steel rebar, corrosion was concentrated around the damaged areas and the number of corroded damage areas remained the same over the test duration. Corrosion occurred at all damage points of the pure enamel coated rebar while only one damage area was significantly corroded on the double enamel coated rebar. The impact-induced damage to the double enamel coating was likely limited to the outer layer and the intact inner layer still served as a physical barrier to corrosion. For the 50/50 enamel coated rebar, the number of damage areas corroding increased with immersion time from 1 at 7 days to all at 84 days. The gradual increase in corrosion area of the 50/50 enamel coating is due to its porous structure consisting of interconnected pores as shown in Fig. 4c.

Table 3 Surface conditions of uncoated and enamel coated rebar at different immersion times

	7 days	28 days	56 days	84 days
Uncoated				
Pure enamel				
50/50 enamel				
Double enamel				

Fig. 9 displays SEM images of the uncoated and enamel coated samples around the impact-induced damage areas. For three enamel coated samples, it can be clearly seen that there was no sign of any under-coating corrosion around the damage points. Therefore, corrosion in enamel coated rebar is generally limited to the vicinity of either existing damage points or coating defects.

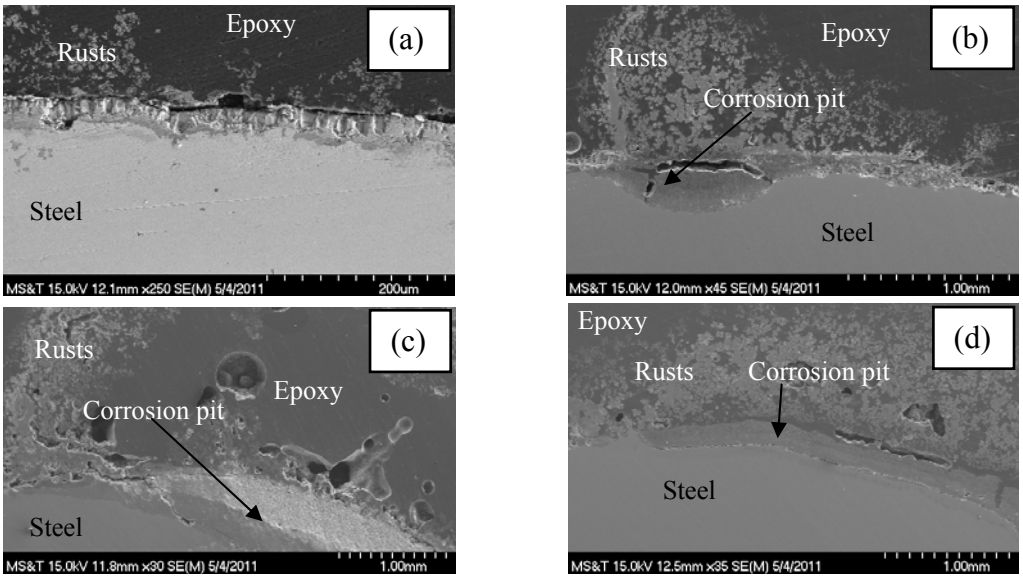

Fig. 9 Microstructure of corroded areas: (a) uncoated, (b) pure enamel coated, (c) 50/50 enamel coated, and (d) double enamel coated sample

Fig. 10 shows the XRD patterns of the powdered rust from various tested samples. It can be seen that Fe_2O_3, Fe_3O_4, α-FeOOH, β-FeOOH, and γ-FeOOH can be detected from the uncoated sample [9] and α-FeOOH, β-FeOOH, and γ-FeOOH are the main compounds of the rusts collected from the coated samples. The relative intensities of these compositions are different among various coating samples because the rust samples were generated under different coating conditions.

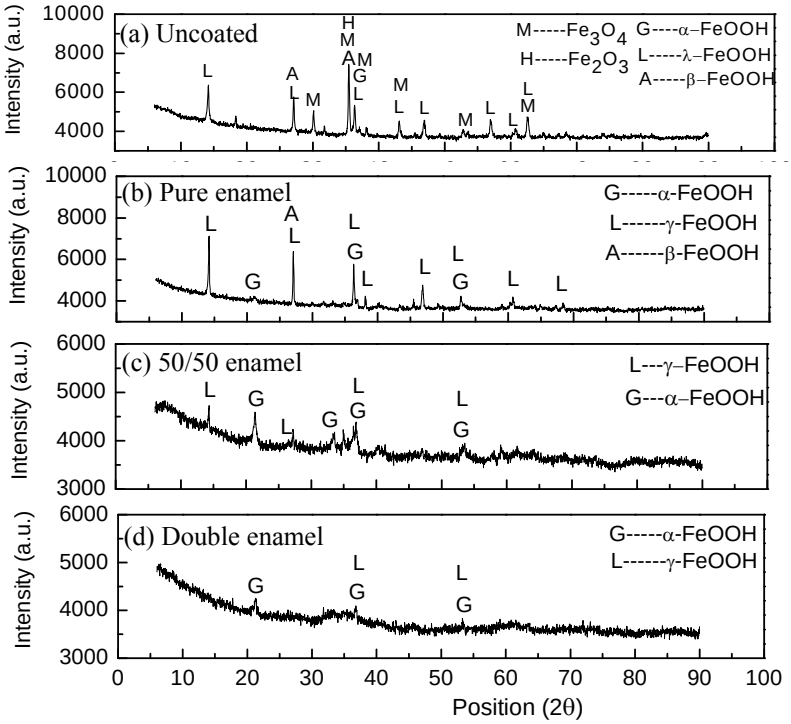

Fig. 10 XRD patterns of rusts generated on uncoated and enamel-coated rebar

Conclusions

Based on the extensive experimentation and analyses, the following conclusions can be drawn:

1. Enamel coatings increase corrosion resistance of steel rebar. Both the pure and double enamel coatings outperform the 50/50 enamel coating due to the interconnected pores present in the 50/50 enamel coating as a result of the calcium silicate addition.
2. Prior damage has significant negative influence on the corrosion resistance of pure and double enamel coatings compared to the 50/50 enamel coating, primarily due to the superior performance of the undamaged pure and double enamel coatings. Corrosion of enamel coated rebar is limited to damaged coating areas due to the strong mechanical and chemical adhesion between the enamel coating and its substrate steel.
3. Fe_2O_3, Fe_3O_4, α-FeOOH, β-FeOOH, and γ-FeOOH are the main compounds of the rust samples from uncoated steel rebar compared to α-FeOOH, β-FeOOH, and γ-FeOOH from the coated samples.

Acknowledgements

Financial support to complete this study was provided in part by the U.S. National Science Foundation (CMMI-0900159), by Roesch Inc. under Project No. 00017522, and by the Center for Transportation Infrastructure and Safety at Missouri University of Science and Technology (No. 00018130). The opinions and findings presented in this paper are those of the authors and do not necessarily represent those of the sponsors.

References

[1] G.H. Koch, M.P.H. Brongers, N.G. Thompson, Y.P. Virmani and J.H. Payer. Corrosion costs and preventive strategies in the United States. Report No. FHWA-RD-01-156, NACE International, 2002.

[2] D.G. Manning. Corrosion performance of epoxy-coated reinforcing steel: North American experience. Construction and Building Materials, Vol. 10, No. 5 (1996), p. 349.

[3] A.B. Darwin and J.D. Scantlebury. Retarding of corrosion processes on reinforcement bar in concrete with an FBE coating, Cement and Concrete Composites, Vol.24 (2002), p73.

[4] E. Sistonen, A. Cwirzen, and J. Puttonen, Corrosion mechanism of hot-dip galvanized reinforcement bar in cracked concrete. Corrosion Science, Vol.50 (2008), p3416.

[5] D. A. Jones, Principles and prevention of corrosion, 2nd Edition, 1996, Prentice-Hall, Inc.

[6] V.F. Hock, S.W. Morefield, D.C. Day, C.A. Weiss, Jr. and P.G. Malone, The use of vitreous enamel coatings to improve bonding and reduce corrosion in concrete reinforcing steel. NACE. Paper No. 08220, Corrosion 2008.

[7] NRC. International Critical Tables, National Research Council, Washington, D.C., McGraw-Hill, 1927, p.116.

[8] G.J. Brug, A.L.G. Van Den Eeden, M. Sluyters-Rehbach and J.H. Sluyters, The analysis of electrode impedances complicated by the presence of a constant phase element. Journal of Electroanalytical Chemistry and Interfacial Electrochemistry, Vol.176 (1984), p275.

[9] E. Zitrou, J. Nikolaou, P.E. Tsakiridis, and G.D. Papadimitrious. Atmospheric corrosion of steel reinforcing bars produced by various manufacturing processes, Construction and Building Materials Vol.21 (2007), p1161.